Revealing hidden pore structure in nanoporous thin films using positronium annihilation lifetime spectroscopy

Hua-Gen Peng, William E. Frieze, Richard S. Vallery, and David W. Gidley[a)]
Department of Physics, University of Michigan, Ann Arbor, Michigan 48109

Darren L. Moore and Richard J. Carter
LSI Logic Corporation, 23400 NE Glisan Street, Gresham, Oregon 97030

(Received 18 November 2004; accepted 1 February 2005; published online 14 March 2005)

The highly inhomogeneous pore morphology of a plasma-enhanced-chemical-vapor-deposited ultralow-k dielectric film ($k=2.2$) has been revealed using depth-profiled positronium annihilation lifetime spectroscopy (PALS) combined with progressive etch back of the film surface. The film is found to have a dense surface layer, an intermediate layer of 1.8 nm diameter mesopores, and a deep region of ~3 nm diameter mesopores. After successively etching of the sealing layer and the isolated 1.8 nm pore region, PALS reveals that the underlying large pores are highly interconnected. This inhomogeneous pore structure is proposed to account for observed difficulties in film integration. © *2005 American Institute of Physics*. [DOI: 10.1063/1.1886905]

There is a great deal of interest in engineering pore characteristics at the nanometer level in thin films for catalysts, gas sensors, selectable permeation membranes, barriers, and low-dielectric constant (low-k) insulators.[1] In ultralow-k (ULK) films for future use in microelectronics, aggressive incorporation of 1–10 nm pores can drive dielectric constants below 2.0.[2] However, increases in pore size and pore density can lead to a network of interconnected pores that provide readily available diffusion paths for damaging process chemicals during integration. As a result, knowing the pore morphology *throughout* such low-k films (even beneath a diffusion barrier) is critical to understanding integration damage associated with photoetching trenches that extend through the entire dielectric. In this letter, we show how depth-profiled positronium annihilation lifetime spectroscopy (PALS), augmented with etch thinning, reveals the complete depth-dependent pore structure of a low-k nanoporous thin film.

A common method for low-k film fabrication is chemical-vapor deposition (CVD). By codepositing a porogen molecule with the dielectric precursor,[3] pores are generated in the film upon release of the porogen during a postdeposition treatment. Several postdeposition treatment processes have been reported, including annealing and plasma, electron-beam (e-beam), and ultraviolet curing.[4] The potential risks of such treatments include the collapse of pores in a surface layer, greater pore interconnection, and an inhomogeneous pore distribution through the film, all of which will complicate the integration of the film. Figure 1 demonstrates the vulnerability of a CVD SiCOH film to trench etching and ashing. Voids in the dielectric and bowing of the trench sidewalls appear consistently at the lower depths of the trenches. Depth-profiled PALS (with etch-back thinning) on similar blanket (unpatterned) films will reveal that the origin of this localized integration damage is clearly correlated with the local pore structure of the film.

Blanket films of SiCOH with dielectric constant $k=2.2$ were prepared in a parallel-plate low-pressure CVD tool using a two step process. The first step involved plasma-enhanced-CVD (PECVD) of the SiOCH film backbone and organic porogens using an oxidative-organosilane discharge at 30 °C. The second step used a high-temperature (400 °C) postdeposition annealing under a plasma discharge, in which the porogen was decomposed and evolved from the film, leaving the SiCOH lattice and yielding a porous film. Control of the plasma annealing conditions allowed tuning of k from 3.0 down to about 2.0. The thickness of the postannealed film is about 620 nm as measured by ellipsometry.

Beam-based PALS is used to analyze the pore structure of the intact film, where a focused monoenergetic beam of positrons is implanted and forms positronium (Ps, the electron-positron bound state) by electron capture.[5] Ps inherently localizes in the pores where its intrinsic vacuum lifetime of 142 ns is reduced by annihilation with molecular-bound electrons during collisions with the pore surfaces.[6] The collisionally reduced Ps lifetime is well calibrated with void size.[5] The detection of Ps annihilating in the vacuum with 142 ns is the telltale sign of Ps diffusing through an interconnected porous network and escaping into a vacuum after as many as one million collisions.[7] PALS depth profil-

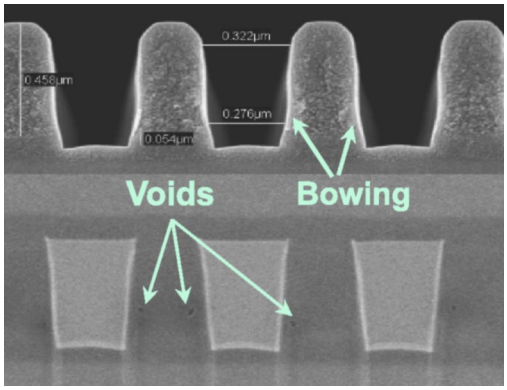

FIG. 1. Cross-sectional scanning electron microscope image of a 0.25 μm trenches etched and ashed in SiCOH low-k (upper half) over one complete level metal structure (lower half) showing that the deeper sidewalls are damaged (bowing and voids) more severely than the upper part of the sidewalls.

[a)]Electronic mail: gidley@umich.edu

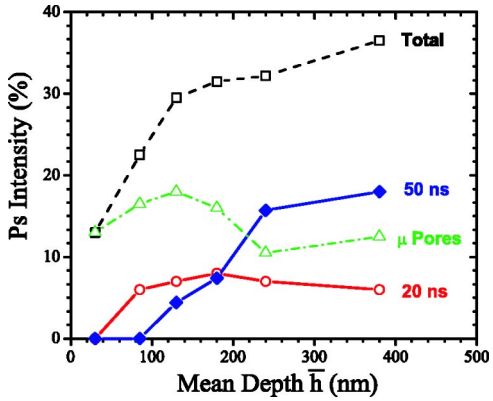

FIG. 2. The intensity of Ps lifetime components fitted for the PECVD SiCOH film as a function of positron mean implantation depth $\bar{h}$. The intrinsic micropore Ps intensity (Δ) is the sum of the 2 ns and 6 ns intensities.

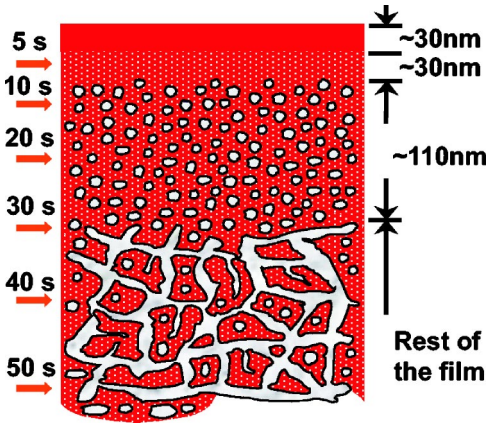

FIG. 3. Cartoon of the pore structure deduced using PALS data on the PECVD SiCOH film of $k=2.2$. A layered structure is assumed with deduced thicknesses displayed along the right side. White dots represent sub-nm micropores. Small (isolated) mesopores and large (interconnected) mesopores are shown below a sealing layer. The arrows on the left indicate the approximate positions of the exposed surface after the corresponding time of etching.

ing is achieved using the well-documented method of varying the positron implantation energy to control the average implantation depth.[8] The typical implantation profile (derivative of a Gaussian) is bell shaped with the full width half maximum roughly equal to the mean implantation depth, $\bar{h}$. The intact SiCOH film was probed with six positron beam implantation energies: 1.1, 2.1, 2.5, 3.0, 4.1, and 5.0 keV, corresponding to mean implantation depths of $\bar{h}=30$, 85, 130, 180, 240 and 380 nm (Ref. 8) for this film of average density $\sim 1.1\ \mathrm{g/cm^3}$.

PALS analysis of the intact blanket film shows no indication of Ps escape into the vacuum at any implantation energy. Hence, either the pores are not interconnected or the surface is sealed, effectively forming a diffusion barrier. In fitting the PALS spectra of the intact film, four Ps lifetime components are required to account for the pore structure at various depths. The two smallest and ubiquitous lifetimes of 2 ns and 6 ns correspond to intrinsic micropores of the SiCOH film. This was confirmed through PALS analysis of a "dense" SiCOH film with $k=3.0$ that presents only these two lifetimes corresponding to defects in the amorphous SiCOH backbone of 0.6 and 0.9 nm in diameter (using the standard Tao-Eldrup model).[6] The third and fourth Ps components with lifetimes of 20 ns and 50 ns are induced by postdeposition removal of the organic porogen and would correspond to diameters of 1.8 nm and 3.5 nm using a spherical pore model.[6] If these porogen-induced pores are interconnected, a more physical cylindrical pore model would yield cross-sectional diameters of 1.5 nm and 2.8 nm. However, we cannot conclusively determine underlying pore interconnectivity from the intact film alone if the surface has any kind of a sealing barrier layer that precludes Ps escape into the vacuum.

Quantitative analysis of the depth-dependent pore structure in the intact SiCOH film involves using a layered model to account for the fitted Ps intensity variations in $\bar{h}$ for the four Ps lifetime components (see Fig. 2). At $\bar{h}=30$ nm (with Ps formation to a depth of ~ 60 nm) only the two intrinsic micropore Ps components are detected, i.e., the surface has a dense layer without porogen-induced mesopores. The 20 ns component first appears at $\bar{h}=85$ nm, however, with deeper implantation the intensity of this component increases only slightly and then decreases. The 50 ns component does not even appear until $\bar{h}=130$ nm, whereupon its intensity increases and levels off after $\bar{h}=240$ nm. Another notable feature in Fig. 2 is that the total Ps intensity is not constant. Particularly at $\bar{h}=30$ nm, the total Ps intensity is only one-half of the asymptotic maximum. The monotonic increase of the total Ps intensity with $\bar{h}$ might be explained by the increase of the porosity over the depth. In a naive two-layer model, it suggests a 30 nm surface layer devoid even of micropores (presumably due to ion-induced pore collapse in the reductive plasma discharge).[9] It should be noted that the film chemistry of the surface layer is also different from the rest of the bulk; it has significantly less carbon and slightly more hydrogen. Chemical modification can also change the Ps formation fraction. Regardless, the dense, top 60 nm act as a sealing layer for any Ps diffusion into the vacuum.

The deduced depth-dependent pore morphology of this intact SiCOH film is depicted in Fig. 3. It has nominally four layers (at least three are required). The first ~ 30 nm layer is a dense (and chemically modified) layer, which forms less overall Ps than the rest of the film. The subsequent layer is of similar thickness with only intrinsic micropores. The third layer of ~ 110 nm is embedded with small and *presumed* isolated porogen-induced pores of 1.8 nm in diameter. The bottom layer is dominated with larger pores and we have drawn them as interconnected pores, however PALS cannot determine the interconnectivity of any of the mesopores underneath the sealing layer. To reveal hidden pore morphology, we have successively etched back the thickness of the film, stopping after each etch step to acquire PALS spectra with each new uncovered surface. We cross check our PALS depth profiling but more importantly, this allows us to probe for pore interconnectivity layer by layer.

Etch-back thinning of the intact film used a capacitively coupled dual-high-frequency discharge with a fluorinated carbon gas chemistry ($\mathrm{CHF_3/CF_4/N_2}$/1000 W source/500 W bias/75 mT). The film was progressively etched to give films of decreasing thickness by controlling the etch time from 5 to 50 s. The Ps escape fraction, the intensity ratio of Ps in a vacuum to the total Ps formed in porogen-induced pores, is plotted against the reduced film thickness for the etched films in Fig. 4. Considering the

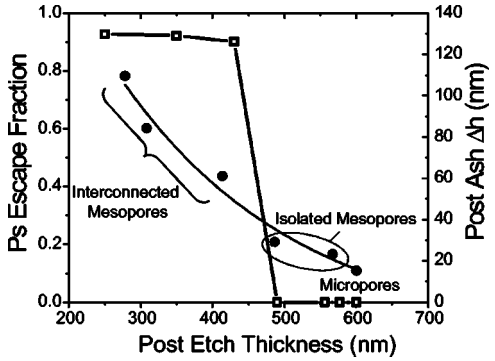

FIG. 4. The Ps escape fraction (at $\bar{h}=85$ nm) (open squares) and the postash film thickness change, Δh (solid circles), for PECVD SiCOH vs the remaining film thickness after varying etch times.

initial thickness of the film is 620 nm, Fig. 4 indicates that at least the top 110 nm of the film is perfectly sealed with no Ps escape into the vacuum, i.e., even the pores characterized by 20 ns Ps lifetime are closed. However, after removal of ~170 nm, almost all the Ps is escaping, indicative of fully interconnected pores in the remainder of the film. Etching therefore confirms our presumption of *closed* 1.8 nm pores in the third layer and highly *interconnected* large pores at the bottom of the dielectric as depicted in Fig. 3.

Considering the porosity profile depicted in Fig. 3, the origin of the integration damage in Fig. 1 can be understood. The large interconnected pores at the lower part of the film are more easily attacked by ion bombardment during the trench etch and/or plasma ash due to the exposed porous sidewalls with interconnected pores. Evidence supporting the enhanced susceptibility to ash damage of the interconnected porous region is presented in Fig. 4. Although the purpose of the plasma ash is to remove photoresist residue, a finite thickness loss (Δh) of the low-k film is affected due to the physical and chemical nature of the plasma. For a film of constant porosity, the degree of ash-induced film thickness reduction should be independent of the film depth. This is not the case for the 'inhomogeneous' film studied in this work. Etch-thinned SiCOH films were subjected to a reductive N_2/H_2 ashing plasma, and the change in film thickness (Δh) was measured (Fig. 4). The increase in Δh due to the ash process correlates well with the onset of Ps escape into the vacuum through the large interconnected pores. This porous network provides accessible channels for the diffusion of plasma species further into the dielectric resulting in greater thickness reduction and also the kind of damage observed in Fig. 1.

In summary, depth-profiled PALS augmented with etch thinning has revealed the detailed hidden pore structure in a CVD SiCOH film. Early detection of such inhomogeneity in ULK pore structure by PALS can help predict integration problems (e.g., sidewall bowing and voiding). PALS can be used to relate the processing properties of these nanoporous materials to the porous structure, and in return, the guidance provided by PALS to improve the microstructure of materials will assist in the development of ULK materials with uniform pore structure and improved robustness to integration damage.

The authors acknowledge the help of Dr. Youfan Liu at International Sematech for supplying Fig. 1. PALS data acquisition was performed by Ming Liu of the University of Michigan. This work was supported by the National Science Foundation (ECS-0100009) and the Low-K Dielectric Program at International Sematech.

[1] F. Schüth, K. S. W. Sing, and J. Weitkamp, *Handbook of Porous Solids* (Wiley-VCH, Weinheim, 2002).
[2] K. Maex, M. R. Baklanov, D. Shamiryan, F. Iacopi, S. H. Brongersma, and Z. S. Yanovitskaya, J. Appl. Phys. **93**, 8793 (2003).
[3] A. Grill and D. A. Neumayer, J. Appl. Phys. **94**, 6697 (2003).
[4] R. C. Hedden, C. Waldfried, H. J. Lee, and O. Escorcia, J. Electrochem. Soc. **151**, F178 (2004).
[5] J. N. Sun, D. W. Gidley, Y. F. Hu, W. E. Frieze, and S. Yang, Mater. Res. Soc. Symp. Proc. **726**, Q10.5 (2002).
[6] T. L. Dull, W. E. Frieze, D. W. Gidley, J. N. Sun, and A. F. Yee, J. Phys. Chem. B **105**, 4657 (2001) and references therein.
[7] D. W. Gidley, W. E. Frieze, A. F. Yee, T. L. Dull, E. T. Ryan, and H.-M. Ho, Phys. Rev. B **60**, R5157 (1999).
[8] P. J. Schultz and K. G. Lynn, Rev. Mod. Phys. **60**, 701 (1988).
[9] A. Grill and V. Patel, J. Electrochem. Soc. **151**, F133 (2004).